Earth and Planetary Science Letters 479 (2017) 366–376

Contents lists available at ScienceDirect

Earth and Planetary Science Letters

www.elsevier.com/locate/epsl

Salinity stratification of the Mediterranean Sea during the Messinian crisis: A first model analysis

Dirk Simon *, Paul Th. Meijer

Department of Earth Sciences, Utrecht University, The Netherlands

ARTICLE INFO

Article history:
Received 22 April 2017
Received in revised form 22 September 2017
Accepted 25 September 2017
Available online 12 October 2017
Editor: M. Frank

Keywords:
ocean stratification
box model
deep-water formation
Mediterranean Sea
Messinian Salinity Crisis
halite

ABSTRACT

In the late Miocene, a thick and complex sequence of evaporites was deposited in the Mediterranean Sea during an interruption of normal marine sedimentation known as the Messinian Salinity Crisis. Because the related deposits are mostly hidden from scrutiny in the deep basin, correlation between onshore and offshore sediments is difficult, hampering the development of a comprehensive stratigraphic model. Since the various facies correspond to different salinities of the basin waters, it would help to have physics-based understanding of the spatial distribution of salt concentration. Here, we focus on modelling salinity as a function of depth, i.e., on the stratification of the water column. A box model is set up that includes a simple representation of a haline overturning circulation and of mixing. It is forced by Atlantic exchange and evaporative loss and is used to systematically explore the degree of stratification that results under a wide range of combinations of parameter values. The model demonstrates counterintuitive behaviour close to the saturation of halite. For parameter values that may well be realistic for the Messinian, we show that a significantly stratified Mediterranean water column can be established. In this case, Atlantic connectivity is limited but may be closer to modern magnitudes than previously thought. In addition, a slowing of Mediterranean overturning and a larger deep-water formation region (both in comparison to the present day) are required. Under these conditions, we would expect a longer duration of halite deposition than currently considered in the MSC stratigraphic consensus model.

1. Introduction

The Mediterranean sedimentary record hosts a kilometre-thick salt giant, deposited during the Messinian Salinity Crisis (MSC, Roveri et al., 2014a, and references therein). The occurrence of evaporites indicates that, overall, basin salinity must have been high. Several different evaporitic lithologies are found in outcrops and are interpreted from seismic profiles. Considerable attention has been paid to establishing the stratigraphy of the MSC, both vertically and laterally (e.g., Ochoa et al., 2015; Lugli et al., 2010; Lofi et al., 2011). A stratigraphic consensus model has been proposed (Fig. 1, summarized by Roveri et al., 2014a), which subdivides the MSC into three evolutionary stages, the first two of which are relevant to this study. Stage 1 is, in marginal basins, dominated by cycles of primary selenitic gypsum alternating with marls. The main halite body is thought to be deposited in the deep basin in stage 2 (in association with cumulate and clastic gypsum). This consensus interpretation notwithstanding, much is still uncertain for the simple reason that most of the deposits are hidden from scrutiny below the present sea (e.g., Roveri et al., 2016). It is therefore difficult to establish a definitive correlation between marginal sequences studied in the field and the deep record as seen in seismics. While the halite mined on Sicily is commonly considered an exposed representative of the deep-basin record (the only, in fact), this is also uncertain. In the consensus model (Roveri et al., 2014a) the halite basin of Sicily is considered an intermediate-depth basin.

Given that the different evaporitic facies correspond to different salinities of the waters from which they precipitated (e.g., Warren, 2016), it would help to have insight from physics as to which spatial distribution of salinity is most likely at any one point in time. Is it possible that the shallow waters of the marginal basins reside at gypsum saturation while, at the same time, the deeper waters reach levels high enough for halite precipitation? Or, are there reasons to expect the basin to be always well mixed? In the latter case, primary selenitic gypsum in marginal basins and halite in the deep basin are not expected to be lateral equivalents and the physics would support the consensus model (Fig. 1).

In the literature one almost exclusively finds qualitative ideas about the spatial distribution of salinity during the MSC. An early

* Corresponding author.
E-mail address: d.simon@uu.nl (D. Simon).

https://doi.org/10.1016/j.epsl.2017.09.045
0012-821X/

example (Sonnenfeld and Finetti, 1985) suggests various precipitation cycles in which gypsum forms in the shallow parts of the basin and halite at greater depth. More recently this configuration was envisaged by de Lange and Krijgsman (2010), who present a chemical mechanism that allows for synchronous deposition of gypsum at the surface and dolomite at depth and take stratification to be more stable due to the presence of deep brines. Roveri et al. (2014b) numerically simulate the notion that cascading explains the Messinian erosional surface and forms deep supersaturated brines. Also Yoshimura et al. (2016) propose that the deep basin is density stratified and that halite-oversaturated brines transport salt from the margins to depth. While Meijer (2006) and Topper and Meijer (2013) investigated the effect that an imposed stratification has on their model results for the MSC, they did not study how and whether stratification arises in the first place.

The purpose of this paper is to gain quantitative, physics-based, understanding of the factors that controlled the vertical distribution of salinity in the Messinian brine basin. For this we use a simple box model. Although general circulation models (e.g., Topper and Meijer, 2015) certainly provide insight about stratification, their long computation time and the extreme ocean salinity during the MSC preclude their use for our purposes. These limitations do not affect box models and these have proven to be valuable tools for testing the sensitivity of Mediterranean parameters to external forcing. In this first study of this kind we explore a box model that includes a deep-water formation region feeding a basin-wide circulation, which can be thought of as a simple representation of a haline overturning circulation. In addition, exchange with the Atlantic, evaporative surface forcing and mixing within the basin are taken into consideration. The model calculates surface and deep Mediterranean salinity through time, which provides a crude quantitative measure for the degree of stratification. A systematic model analysis allows us to identify under which range of parameters the basin is mixed and when, in contrast, it is stratified. Our findings will be discussed in terms of their potential implications for the stratigraphical relationships within the Messinian sedimentary record. What makes the analysis timely is that industry data of the Levant basin have become available (e.g., Feng et al., 2016) and that the scientific community is working towards drilling the deep Messinian record (e.g., MEDSALT initiative, https://medsalt.eu).

2. Model description

Consider the following thought experiment: an ocean basin subject to evaporation is represented as a single water column. The evaporation will cause salinity of the surface water to increase. As a result, surface density is enhanced and a gravitational instability is created, which leads to mixing of the water column. As long as evaporation continues, these steps will repeat themselves and the column will be essentially homogeneous at all times. This effect is exemplified by the recent Dead Sea, apart from the fact that here a stable stratification is installed seasonally due to heating (e.g., Sirota et al., 2016). We learn from this thought experiment that, in order to create persistent (i.e., lasting longer than one year) stratification, a single-column representation does not suffice and that lateral variation is crucial.

In this study we use a box model, as show in Fig. 2. In the Mediterranean Sea evaporation exceeds precipitation and river input. We denote net evaporation as e and take it to act uniformly across the basin. Exchange with the Atlantic adds "fresher" water to, and removes saltier water from, the Mediterranean Sea at its western side. Instead of considering the drivers of exchange – Atlantic-Mediterranean density difference and the gateway dimensions (e.g., Simon and Meijer, 2015) – we prescribe a value for the

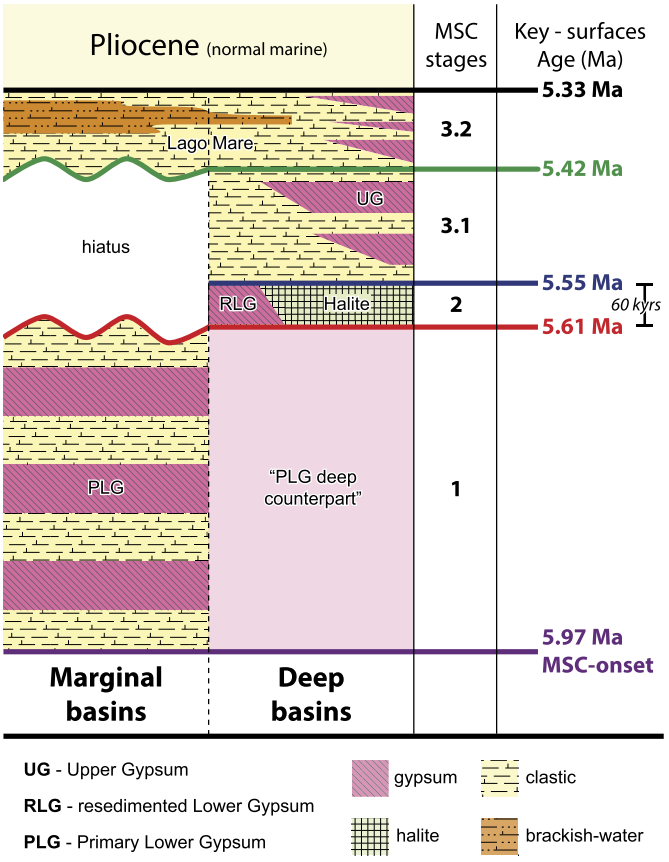

Fig. 1. The MSC stratigraphic consensus model (linear in time), simplified from Roveri et al. (2014a). (For interpretation of the references to colour in this figure, the reader is referred to the web version of this article.)

outflow from the Mediterranean (q). Volume conservation then implies the Atlantic inflow equals ($q + e * A$).

Wåhlin and Cenedese (2006) investigate the response of ocean stratification to the inflow of dense water from an adjacent marginal sea by solving the advection–diffusion equation which allows them to obtain a continuous depth variation of water properties. As a first step towards this, we consider the simpler case where the basin is divided into a surface layer (subscript "*Surf*") and a deep layer (subscript "*Deep*"). Turbulent mixing between the surface and deep box is represented as a diffusive process, following the models for the Mediterranean Sea of Tziperman and Speer (1994) and Matthiesen and Haines (2003). Mixing is controlled by a constant diffusivity κ and a vertical length scale equal to the vertical distance between the middle of the two layers.

In the present-day Mediterranean circulation (e.g., Tsimplis et al., 2006), Atlantic surface water flows towards the east and increases in salinity due to evaporation. In the Levantine basin the water becomes dense enough to sink to intermediate depth, at which level it spreads westwards throughout the basin. On its path to the west, the salt-preconditioned water passes through regions where it is subjected to cold and dry winds (e.g., Schroeder et al., 2012). This leads to further increase in density and forms deep water. Modern deep-water formation occurs at the northern rim of the Mediterranean Sea in shallow, restricted, basins, like the Adriatic Sea or the Aegean Sea, and in open-ocean convection sites (e.g., Gulf of Lions). The dense water produced charges the Mediterranean overturning circulation. In our model the *deep-water formation*-box (*DWF*) represents such a region. The production of deep water (to which we will refer as "convection") is parametrised as a constant volume flux w. The same volume of water per unit of time is advected upwards outside the DWF. Con-

vection and advection together lead to a simple basin-wide circulation (Fig. 2).

When the DWF-box reaches halite saturation, which we define to be when $S_{DWF} = 350$ g/l, halite starts to crystallize, causing halite rain into the deep box (e.g., Yoshimura et al., 2016; referred to as "rain from heaven" in Warren, 2016). In the deep box it may partly or entirely re-dissolve and the remainder is removed from the system by sedimentation. How much of the halite raining down is re-dissolved is set by the factor c ($c = 0$, no re-dissolution; $c = 1$, full re-dissolution). All halite that forms in the deep box (when $S_{Deep} = 350$ g/l) is deposited equally across the Mediterranean surface (A), allowing us to estimate its sedimentation rate (cm/yr) under the assumption of a uniform density for the halite (2160 kg/m^3). Because, in reality, the deposits are unlikely to cover the entire surface area of the basin, our sedimentation rate is a conservative estimate.

The salt concentration of the three boxes evolves as:

$$V_{Surf}\frac{dS_{Surf}}{dt} = q * \Delta S_{AltSurf} + w * \Delta S_{DeepSurf} + e * \left(A * S_{Atl} - A_{DWF} * S_{Surf}\right) - \kappa * A_{Surf} * \frac{\Delta S_{SurfDeep}}{0.5 * V/A} \quad (1)$$

$$V_{DWF}\frac{dS_{DWF}}{dt} = w * \Delta S_{SurfDWF} + e * A_{DWF} * S_{Surf} - dDWF_{sink} \quad (2)$$

$$V_{Deep}\frac{dS_{Deep}}{dt} = w * \Delta S_{DWFDeep} - \kappa * A_{Surf} * \frac{\Delta S_{DeepSurf}}{0.5 * \frac{V}{A}} + c * dDWF_{sink} - dDeep_{sink} \quad (3)$$

The subscript "Atl" stands for the Atlantic. S represents the salinity and $\Delta S_{xy} = S_x - S_y$. The limitations imposed on our model as a result of the various assumptions and simplifications will be treated in the discussion (Section 4).

3. Model analysis and results

3.1. Setup of the analysis

With the model outlined in the previous section we systematically explore the effect on salinity and salinity stratification of all parameters. Only basin volume and surface area are kept constant. Since the late Miocene hypsometry was already close to that of the present day (Meijer and Krijgsman, 2005), we set the volume and surface area of the entire box-system to modern values ($3.75 * 10^{15}$ m^3 and $2.48 * 10^{12}$ m^2). In order to allow for a clear presentation of our findings, we will first present only a subset of the experiments (Figs. 3–8), followed by a summary (Fig. 9). We start by reporting the impact of different strengths of flux-related parameters (Section 3.2). This is followed by the relevance of the box sizes and the extent of re-dissolution of halite rain in the deep basin (Section 3.3). Section 3.4 summarises all findings, which sets the basis to form implications for the MSC (Section 4).

Three net evaporation values ($e = 0.25$ m/yr, 0.5 m/yr, 1.0 m/yr) are tested. These cover the range of estimates for the late Miocene (e.g., Simon et al., 2017; Gladstone et al., 2007). For reference, the present-day value amounts to ~0.5 m/yr (Mariotti et al., 2002). If we consider a single-box representation of the Mediterranean and combine the conservation of salt mass (e.g., Fig. 2 of Simon and Meijer, 2015) with the conservation of water mass, it is straightforward to calculate the outflux q required to increase salinity to large values (the expression for q reads $q = eS_{Atl}/\Delta S_{MedAtl}$, e.g., Bryden and Stommel, 1984). For the three e values considered, halite saturation ($S_{Med} = 350$ g/l) would be reached for a q of

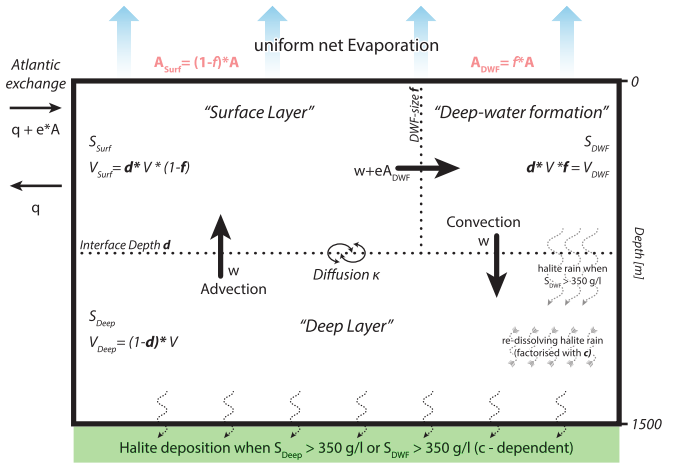

Fig. 2. Illustration of all parameters in the box model (e.g. salinity, volume, area or halite rain). The basin is split up into three boxes ("Surf", "DWF" and "Deep"). Parameters, related to water fluxes, are represented as arrows (not to scale). (For interpretation of the references to colour in this figure, the reader is referred to the web version of this article.)

0.002 Sv, 0.004 Sv and 0. 009 Sv, respectively. These are clearly much lower than the present-day exchange at Gibraltar, which has an annual mean of about 0.7–0.8 Sv (Soto-Navarro et al., 2010). In our sensitivity analysis we consider three values for q (0.001 Sv, 0.01 Sv, 0.1 Sv). This is followed by results related to the vigour of circulation (w) and mixing (κ). It is difficult to identify a single number for annual mean present-day overturning. However, zonal overturning streamfunctions based on observations (e.g., Sevault et al., 2014) and on modelling (Mikolajewicz et al., 1993; Topper and Meijer, 2015; Grimm et al., 2015) indicate strength of the order of 1–2 Sv. Slightly weaker deep-water formation fluxes (mostly between 0.1–0.6 Sv) are reported by Béranger et al. (2010). Our analysis shows that $w > 0.1$ Sv will never yield significant stratification, which, in fact, is a first important result. We thus consider lower values ($w = 0.1$ Sv and 0.01 Sv, Figs. 3–5). We test the mixing strength for κ values of 10^{-5} m^2/s (Figs. 3 and 4) and 10^{-4} m^2/s (Fig. 5). These values have been inferred for the general background mixing of the global ocean interior (e.g., Jayne, 2005; Munk, 1966) and have been applied in other studies of the Mediterranean (e.g., Tziperman and Speer, 1994). The flux-related parameters are explored for the case of a surface layer thickness of 160 m ($d = 160/1500$), a DWF-box with a surface area that is 1/3 of the entire Mediterranean area ($f = 1/3$) and full re-dissolution of halite in the deep basin ($c = 1.0$; Figs. 3–5). This specific combination of settings is chosen as our starting point because it allows for the best visual presentation of the model behaviour. The effect of $c < 1.0$ will be investigated in second instance, together with that of other values for d and f.

Figs. 3–8 present changes in time of salinity of the three boxes (S_{Surf}, dashed; S_{DWF}, solid, S_{Deep}, dotted) and the degree of stratification (shaded). Each simulation is calculated for a different set of parameters. Fig. 3 shows a matrix of experiments with a different e in each column and different q in each row.

3.2. Sensitivity of salinity to flux-rated parameters

All our model experiments start at a salinity of 36 g/l, which is about equal to the salinity of the presently inflowing Atlantic water. Through time, salinity in the basin will increase due to the net evaporative loss and the restriction from the Atlantic. The salinity in the DWF-box evolves consistently to be the highest of all boxes, because the water in this box has been subject to evaporation the longest. The second highest salt concentration is hosted

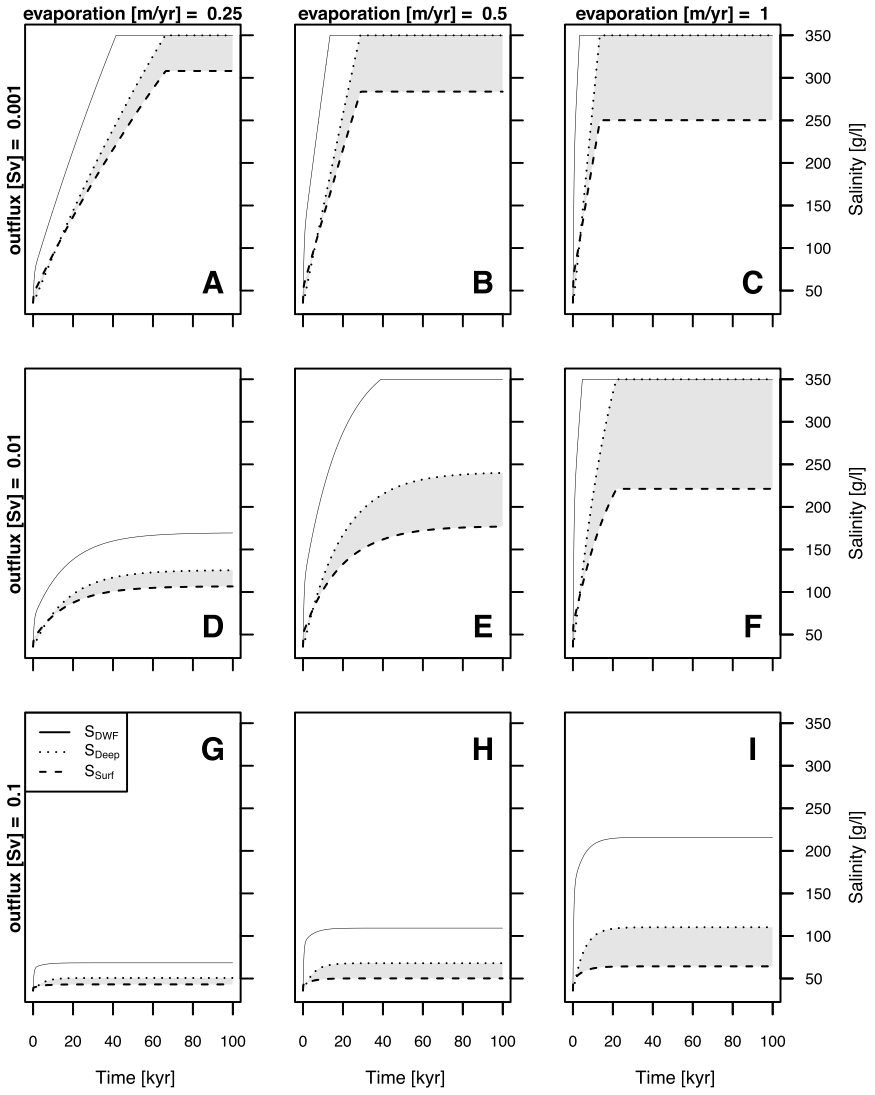

Fig. 3. All nine panels follow the same layout and model setup ($f = 1/3$, $d = 160/1500$, $c = 1.0$). The experiments plotted in each column of panels are forced with a different net evaporative forcing (0.25 m/yr, left; 0.5 m/yr, centre; 1.0 m/yr, right). The experiments plotted in each row are forced with a different exchange flux with the Atlantic (0.001 Sv, top; 0.01 Sv, middle, 0.1 Sv, bottom). The diffusivity κ is set to a value of 10^{-5} m^2/s and con-/advection w is 0.01 Sv. The x-axis is time and the y-axis is salinity. Each line represents one box of our model (Fig. 2): Deep-water formation (DWF), solid line; Deep, dotted line; Surface, dashed line. The salinity difference between surface and deep box is the "degree of stratification" (shaded in grey).

by the deep box, because it is directly fed by the DWF-box. The lowest salinity is reached by the surface box, because it is under the most direct influence of the Atlantic exchange.

Figs. 3G, 3H and 3I show that greater evaporation leads to faster salinity increase and to higher equilibrium salinity in each box. The degree of stratification is also greater for a larger evaporation, because the salt concentration in the deep box is impacted more than surface salinity. This holds true for all panels presented. However, when the deep basin reaches halite saturation, the deep salinity stays constant, but the surface water is fresher for stronger evaporation (Figs. 3A, 3B, 3C). This is because a greater e will increase the Atlantic inflow, which increases the salt intake by the basin as a whole, but dilutes the surface layer. Steady state is reached fastest for low evaporation values, when water does not saturate for halite (comparing Figs. 3G to 3I). This trend would continue if salinity were allowed to rise indefinitely. However, when a box reaches 350 g/l its salinity is capped, forcing the system to steady state at that instant (time-dependent terms on the left-hand side of equations (1)–(3) go to zero). Therefore, when S_{DWF} is at 350 g/l, steady state is reached fastest for high evaporation values.

Comparing Figs. 3A to 3D and 3G shows that a smaller exchange causes salt concentration in all boxes to reach higher values (also observed by comparing Figs. 3B with 3E and 3H and 3C with 3F and 3I). Similar to the response to evaporation, variation of the exchange impacts the deep box stronger than the surface box, causing greater stratification for smaller q values. This holds true until the deep basin hits halite saturation. That moment S_{Deep} is fixed, a lower q can only further raise S_{Surf}, leading to a decreased stratification (compare Figs. 3I to 3F and 3C, for example). This demonstrates that the value of Atlantic exchange that causes the deep basin to just reach to halite saturation will create the strongest stratification. The exact magnitude depends on the value of the other model parameters (see Fig. 9 and supplementary Figs. S11–S13, which will be discussed in Sections 3.4 and 4). When exchange is restricted, more time is needed to reach equilibrium (when $S_{Deep} < 350$ g/l, compare D and G in Fig. 3). For $S_{Deep} = 350$ g/l, the opposite is the case (compare C and F in Fig. 3).

To evaluate the effect of circulation on salinity, we add to Fig. 3 an additional set of experiments with a larger w value (red in Fig. 4). Stronger advection causes faster redistribution of salt, lead-

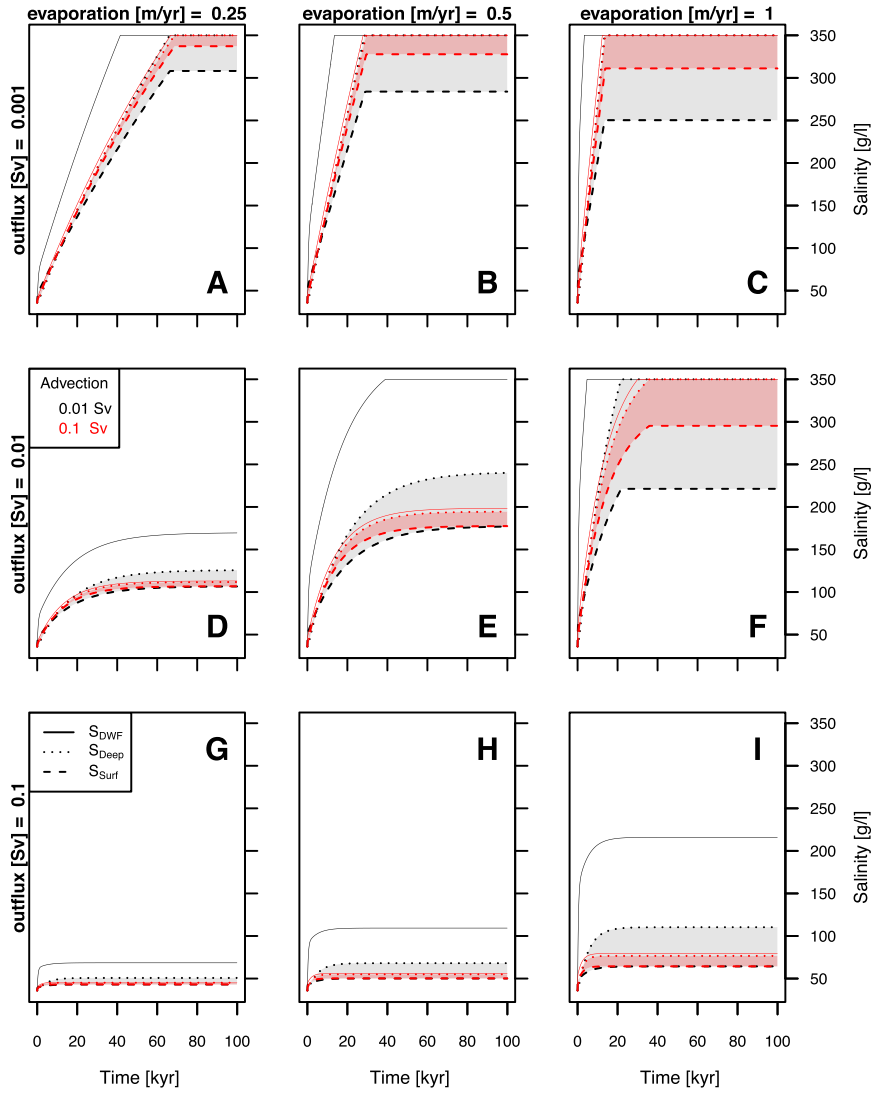

Fig. 4. Presented experiments have an identical setup to the ones in Fig. 3. However, per panel, two experiments are shown with different advection fluxes (0.01 Sv, black; 0.1 Sv, red). (For interpretation of the references to colour in this figure legend, the reader is referred to the web version of this article.)

ing the salinity of the boxes to approach each other (i.e. reduced stratification). Again, the reaching of halite saturation will change the response to this parameter. When $S_{DWF} < 350$ g/l, the surface salinity is not affected by the magnitude of w; however, the deep salinity is and it is larger for smaller w, causing greater stratification (e.g., Fig. 4I). When $S_{DWF} = 350$ g/l (e.g., Fig. 4C), only the surface salinity is affected and is lower for smaller w values, causing enhanced stratification. Time to equilibrium is hardly affected by the circulation strength. Larger w values cause salinity to reach equilibrium earlier, when $S_{DWF} < 350$ g/l. A reversed behaviour is seen in the case, when $S_{DWF} = 350$ g/l.

The experiments in Fig. 5 have an identical setup to experiments in Fig. 4 but correspond to a larger κ of 10^{-4} m^2/s representing increased mixing. Larger values of κ decrease the difference in salinity between the surface and the deep basin (i.e., lead to lower stratification). S_{DWF} is hardly impacted by κ (compare Figs. 4A with 5A). Less mixing leads to greater S_{Deep} (when $S_{Deep} < 350$ g/l, S_{Surf} is not affected) and to lower S_{Surf} (when $S_{Deep} = 350$ g/l). If the water column is particularly stable, an even less restricted gateway could lead to significant stratification (mixing very weak, $\kappa = 10^{-6}$ m^2/s, see supplementary Fig. S10). The time to equilibrium, although hardly impacted, is reached faster when κ is larger.

3.3. Effect of variation of d, f and c

Following the analysis on the response to flux-related parameters, we now consider how the established insight is affected by other choices for the parameters d, f and c. For the sake of clarity, we choose one experiment from Fig. 3 and consider how it is affected by a different horizontal interface depth (d, Fig. 6), DWF-area (f, Fig. 7) and strength of re-dissolution of halite in the deep basin (c, Fig. 8). The selected experiments are chosen so that the impact of d, f and c is clearly illustrated.

The horizontal interface depth impacts the volume distribution of the boxes. The steady-state salinity is independent of the position of d (comparing Figs. 6A with 6B and 6C and 6D with 6E and 6F). Considering equations (1)–(3) it becomes clear that d can only affect the salinity evolution prior to equilibrium. The shallower d is, the longer it takes to reach a certain salinity in both surface and deep box. This is the case because with a shallower d, the deep box has a larger volume, which implies more Mediterranean water needs to be raised in salinity, which takes longer (compare Figs. 6A and 6C). This response of the system to d holds true across the entire parameter space.

The larger the DWF-surface area f, the greater is the calculated degree of stratification (Fig. 7). When $S_{Deep} < 350$ g/l, this

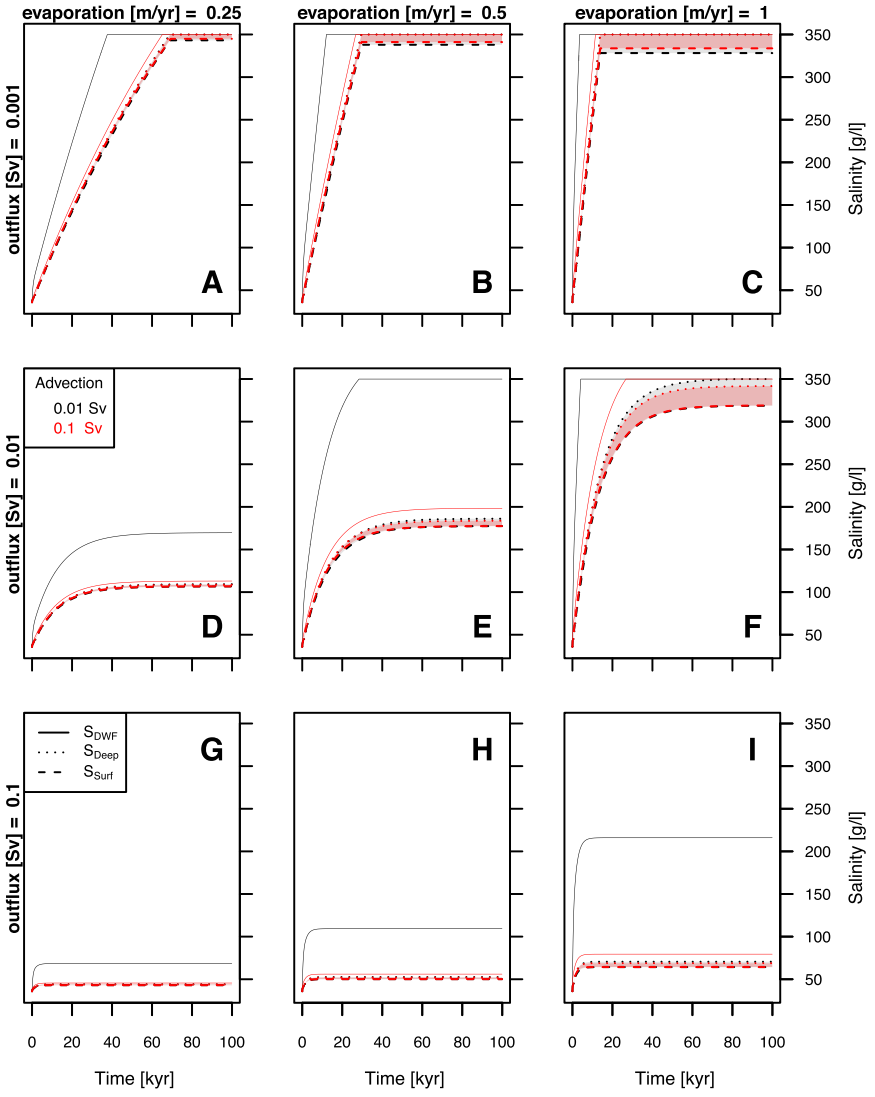

Fig. 5. Presented experiments have an identical setup to the ones in Fig. 4. However the diffusivity κ is set to a value of 10^{-4} m^2/s. Supplementary Fig. S10 plots the same experiments for $\kappa = 10^{-6}$ m^2/s. (For interpretation of the references to colour in this figure, the reader is referred to the web version of this article.)

is because S_{Deep} is larger, while S_{Surf} is relatively constant (compare panels D with E and F in Fig. 7). When $S_{Deep} = 350$ g/l, it is because S_{Surf} is lower, while S_{Deep} is relatively constant (compare panels A with B and C in Fig. 7). This behaviour of the surface salinity makes sense, because even while depositing halite the deep box can recycle salt to the surface via advection.

So far, our results (Figs. 3–7) only considered the scenario in which any halite that crystallizes at the surface is fully re-dissolved in the deep basin. When no or partial re-dissolution occurs, salt is removed from the system by deposition at an earlier stage, leaving the deep basin less saline and therefore leading to weaker stratification (compare Fig. 8A–C). Analysing the response to c also demonstrates that if not all salt is re-dissolved, halite deposition starts earlier (up to several thousand years). Moreover, parameter c affects the described response to circulation. Each panel of Fig. 9 presents results of 10^4 model experiments for a range of w and q values. Panels A and B correspond to $c = 0$ while C and D have $c = 1$. In panels A and C, κ equals 10^{-5} m^2/s and in B and D it is 10^{-4} m^2/s. The other parameters are the same in all experiment panels: $e = 1.0$ m/yr, $f = 0.3$ and $d = 160$ m. The model runs are calculated for 1000 kyrs, rather than 100 kyrs, to guarantee that all experiments reach a steady state. In addition to the level of stratification, we also extract the sedimentation rate at which halite is deposited (indicated by contours), once an experiment reaches steady state. This shows that, when w is approaching zero, the stratification may again decrease slightly (e.g., Fig. 9A). This effect is also there in Figs. 3–5 but not observable because it is overprinted by halite rain re-dissolving in the deep basin.

3.4. Summary of the sensitivity analysis

Strongest stratification occurs when the deep basin just reaches halite deposition and when the surface salinity sits as close as possible to that of the Atlantic. The existence of strong stratification implies a marked distribution of salt within the basin and can involve halite deposition in a situation in which the mean Mediterranean salinity is below halite saturation. An important finding is that our experiments divide into two sets. Depending on whether water passes the saturation threshold, the system demonstrates different sensitivity to the model parameters. For example, if salt concentrations stay below 350 g/l then equilibrium is reached fastest when q is high, e is low and w and κ are high. However, if halite saturation is reached in the deep box, then equilibrium is reached fastest when q is low, e is high and w and κ are low. The reason for this is the salinity capping due to the crystallization of halite.

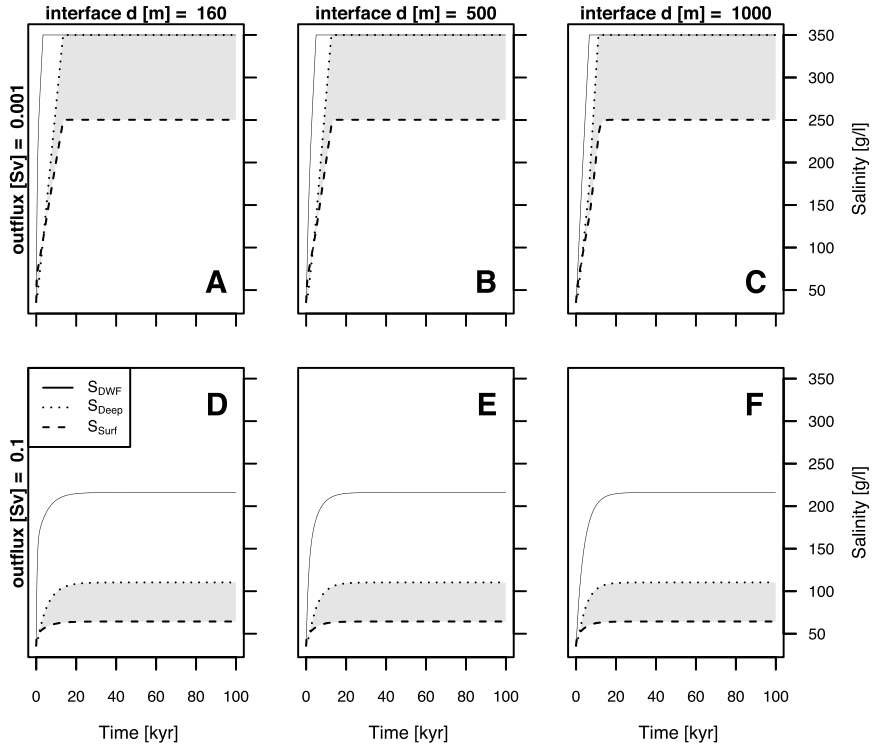

Fig. 6. Panels A and D are identical to Figs. 3C and 3I, respectively. Panels B/E and C/F differ to A/D in value the horizontal interface depth d (B/E, 500 m; C/F, 1000 m).

Fig. 9, together with the supplementary Figs. S11–S13, summarize the system's behaviour in terms of the level of stratification that is reached in steady state. The response to some of the parameters proves to be relatively straightforward: the interface depth has no impact on the level of stratification and stronger evaporation causes stronger stratification. Also, a larger DWF-region (larger f) increases stratification and a stronger mixing, naturally, reduces stratification. The other parameters q, w and c are more complex. Generally, high w and q values create weak stratification and small w and q values cause larger stratification (Fig. 9). However, largest stratification is formed when w and q are just allowing for halite saturation (dependent on the strength of the diffusivity, supplementary Fig. S14). Another interesting observation is that, although for large c only very low q values will cause the deposition of halite (consider contours on Figs. 9C and 9D), for small c also large q values (e.g., present-day) result in deposition when w is small (consider contours on Figs. 9A and 9B). Halite deposition during such a scenario (small c, large q and small w) would entirely be created from halite rain and the deep basin would not be at halite saturation yet.

4. Implications for the MSC

4.1. Was there significant stratification during the MSC?

We now use the model to try and answer the question outlined in the introduction: would we expect significant stratification of the Messinian basin? In order to achieve, for example, a stratification of ∼200 g/l it follows from our analysis that this occurs when evaporation is strong ($e = 1.0$ m/yr), mixing is weak ($\kappa = 10^{-5}$ m^3/s), halite is re-dissolving ($c = 1.0$), deep-water flux is below 0.01 Sv and exchange is between 0.01–0.03 Sv (Fig. 9C). If no halite re-dissolves ($c = 0.0$), a weaker but still significant stratification (e.g., ∼100 g/l) is created, for w in the range ∼0.01–0.04 Sv (Fig. 9A). By halving evaporation ($e = 0.5$ m/yr, supplementary Fig. S11) maximum stratification is reduced by approximately 50% with an exchange range of lower values (∼0.005–0.01 Sv supplementary Figs. S11A and S11C). Such a linear response between evaporation and salinity was previously documented (Simon and Meijer, 2015). These ranges are for a DWF-size of $f = 1/3$. If the two evaporation values are considered for an f value of 0.1, the maximum degree of stratification, which now occurs at when exchange and overturning are approximately halved, is reduced by about 50% (compare Figs. 9 with S11 and Figs. S12 with S13). For parameter values outside the range mentioned here, the stratification is weak or the basin is essentially found to be mixed.

The question now is whether the combinations of parameters we find to be associated with stratification, are to be expected for the Messinian crisis. Recently derived estimates of late Miocene net evaporation in the Mediterranean range between ∼0.79 m/yr and ∼0.88 m/yr (including and excluding the drainage of the Chad-Eosahabi catchment, respectively; Simon et al., 2017). These values are positioned within the parameter range that would allow for significant stratification. Present-day estimates of turbulent diffusivity, as a measure of mechanical mixing, are of the order of $\sim 10^{-5}$–10^{-4} m^2/s (e.g., Jayne, 2005; Munk, 1966). To create significant stratification during the MSC we found that κ needs to be at the lower end of this range. Although corresponding values for diffusivity are not known it has been pointed out that in marginal settings (Bryden et al., 2014) or when strong water column stability is present (e.g., Marzeion and Levermann, 2009), mixing may indeed be minor. If κ is less than 10^{-5} m^2/s, even larger w and q or lower f values than those reported at the start of this section would allow for significant stratification (see supplementary Fig. S14). As to the required reduction in the exchange (down to the order of 0.01 Sv) this can ascribed to the greater constriction of the Messinian gateway. Meijer (2012), Rohling et al. (2008) and Simon and Meijer (2015) addressed the strait dimensions that would be associated with such limited exchange. Thus, with regards to e, κ, and q a significant Mediterranean stratification during the Messinian would seem possible to achieve. However, this is true only if overturning (w) is weak and the size of

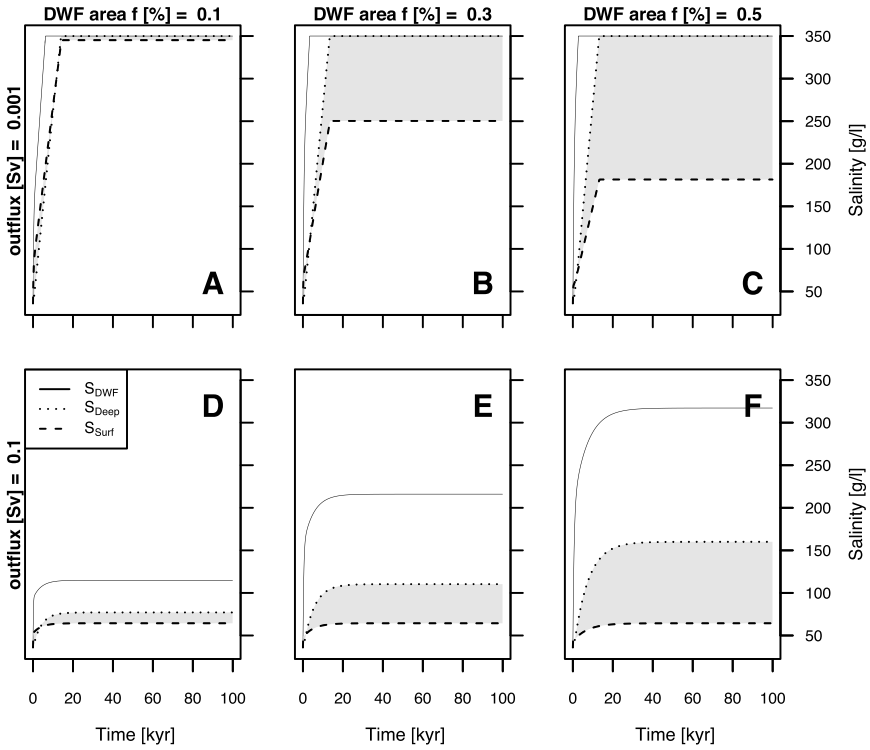

Fig. 7. Panels B and E are identical to Figs. 3C and 3I, respectively. Panels A/D and C/F differ to B/E in value the DWF-size f (A/D, 0.1; C/F, 0.5).

the deep-water formation region (f) is large. If these conditions are not met, the basin is expected to be mixed. Unfortunately, parameters w and f are much harder to constrain for the MSC than the ones already discussed. In itself, the required combination is surprising, because a large f might intuitively not be associated with a small w. The reason for this specific combination is that a large f leads to low surface salinity and high salinity in the DWF box, which is needed to increase the deep salinity and therefore stratification. However, if the salt is transported by water and not as halite rain, only a small amount of water should convect, because it would otherwise lead to a more mixed basin. As to w, if the strength of overturning is at least in part mechanically coupled to the strength of Atlantic exchange then a smaller w would indeed be expected during the Messinian. The alternative, that the overturning is exclusively set by the atmospheric forcing, resulting in a basin that is ever more overmixed when the exchange is reduced, seems unlikely (cf. Topper and Meijer, 2015). Also, to the extent that convection depends on the density difference between DWF and deep box, the moment that both are close to halite saturation, w will be small. The value of f required to obtain significant stratification proves large compared to the value that would describe the present-day area of intermediate and deep-water formation. For reference, the site of open-ocean convection in the Gulf of Lions corresponds to an f of about 0.004 (Herrmann et al., 2009). Taken together, present-day regions of deep mixing do not occupy more than 1% of the Mediterranean surface (e.g., Pinardi and Masetti, 2000; D'Ortenzio et al., 2005; Tsimplis et al., 2006). Starting from a case with strong stratification ($\kappa = 10^{-5}$ m^2/s and $e = 1.0$ m/yr, supplementary Fig. S15), with decreasing f, the parameter space of q and w that leads to significant stratification narrows. When f is below 0.05 only for a diffusivity value lower than 10^{-5} m^2/s, stratification of 50 g/l can be reached. The implication of a relatively large f would be that a large part of the eastern Mediterranean acted like our DWF-box. This would imply that in this region surface waters were very salty, causing, for example, halite rain. Further west, surface waters would decrease in salinity, most likely in gradual fashion towards the Atlantic.

An independent way to decide on the likelihood of stratification during the MSC stems from the fact that the different scenarios prove to imply different sedimentation rates (see also Topper and Meijer, 2013). The consensus model places the Messinian halite layer within a short time period of ~60 ka (Fig. 1, Roveri et al., 2014a) and Ryan (2008) estimates the salt volume to be $\sim 2 * 10^{15}$ m^3. By spreading this volume over the Mediterranean surface area employed in our calculations, we arrive at a salt thickness that can be directly compared to the model results. It proves that the implied sedimentation rate of the order of ~1–2 cm/yr can only be reached for a relatively well-mixed basin (Fig. 9). For a stratified Mediterranean, our results suggest much lower sedimentation rates of below 0.5 cm/yr. In order to explain the observed thickness with such low rates, the duration of halite deposition in the deep basin must have been longer – at least 100–200 kyrs, but possibly even more – than considered in the consensus model (Fig. 1, Roveri et al., 2014a). The reason for this is that greater Atlantic–Mediterranean exchange is needed to create significant stratification (about twice the exchange associated with a mixed basin, and even more for lower κ, supplementary Fig. S14; cf. Flecker et al., 2015). This corresponds to a lower net salt flux from the Atlantic Ocean into the Mediterranean Sea. The insight that a stratified basin results in a lower halite sedimentation rate can already be inferred from Topper and Meijer (2013) who looked at the effect of an assumed stratification (rather than solving for it). Their Fig. 10 shows that the halite thickness created in 60 ka is less for increased stratification which also points to a low rate of sedimentation.

4.2. Comparison to the sicilian record

Our model analysis informs us about the conditions under which the Messinian basin would have exhibited (strong) salinity stratification. In the stratified case it is conceivable that gypsum

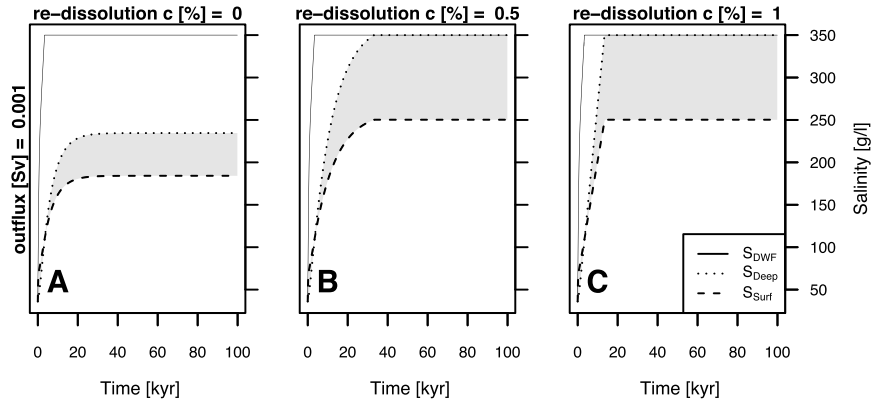

Fig. 8. Panel C is the identical experiment to Fig. 3C. Panels A and B differ to C in the strength of re-dissolution of halite rain c, which is 0.0 and 0.5, respectively.

precipitated from the upper water layer in the shallow parts of the basin, while at the same time halite accumulated in the deep(-er) basin. Thus, from a process point of view, simultaneous deposition of marginal gypsum now assigned to stage 1 (Fig. 1; Roveri et al., 2014a) and halite, appears a possibility. The intermediate-depth Messinian deposits of Sicily display primary gypsum in direct association with the halite: how does this relate to our findings?

Firstly, gypsum cumulates are observed in the Caltanissetta basin at Pasquasia and considered to be a lateral equivalent to the halite (Manzi et al., 2012 and references therein). This may point to the occurrence of strong lateral variation in salinity, not captured by our model. Alternatively, it could be a consequence of (vertical) stratification if we assume that the Pasquasia deposits accumulated at lower depth than the adjacent halite. The observation seems hardest to reconcile with the notion of a basin that has a uniformly high salinity.

Secondly, gypsum occurs as thin anhydrite layers within the halite of the Caltanissetta basin giving it, together with thin shale veneers, a clear rhythmical nature, which has been attributed to seasonal dry-wet oscillations (Manzi et al., 2012). When our model is forced with a changing freshwater budget (Fig. S16) in order to mimic such rhythmic alternations, periodic changes of less ∼200 years are too fast to affect the salinity stratification. However, due to the net freshwater oscillations the salinity of the deep water will drop below the saturation of halite for part of the cycle (Fig. S16), independent of the strength of the water column stability. This would be in agreement with the observed rhythmical nature of the deposits (Manzi et al., 2012).

Of course, these considerations are as yet only based on the Sicily record and it is not known whether the behaviour was widespread throughout the basin or whether the envisaged temporal variation in salinity also extended down into the truly deep basin.

5. Discussion

5.1. The neglect of temperature

The relative importance of salinity and temperature in controlling seawater density is determined by the ratio of the coefficients of haline contraction to thermal expansion which is typically about 4:1 (e.g., Johnson et al., 2007). Present-day temperature in the Mediterranean ranges from ∼10 °C during winter in the northern Adriatic Sea to ∼30 °C during summer in the Gulf of Sirte or the Levantine Sea (Rohling et al., 2015). If this temperature span would be imposed as a variation at a single location at the surface, the density would change by an amount equivalent to a change in surface salinity of ∼5 g/l. Present-day salinity in the Mediterranean ranges from ∼35 g/l in the northern Adriatic or Aegean Sea to ∼40 g/l in the Levantine Sea (Rohling et al., 2015) and it follows that temperature and salinity both play a role. However, during the MSC the salt concentration reached up to absolute values of ∼350 g/l, while the Atlantic and rivers added much fresher water (∼36 g/l or less). With increasing temperature the haline contraction coefficient decreases and the thermal expansion coefficient increases (Thorpe, 2005). Despite the fact that its waters have a particular chemical composition, the Dead Sea could be an interesting analog to the MSC. Anati (1997) reports that measurements of the Dead Sea water yield a ratio of 2:1 between haline contraction to thermal expansion. Although it is unknown what is the appropriate value for these coefficients for the MSC, the very ranges of temperature and salinity imply that the latter dominated over the former. The role of temperature will not be negligible in a situation where the water column is close to being homogeneous in salinity. Even when salinity is very high, variations in temperature of the surface water would be significant in that they determine the stability. This behaviour has been documented in detail for the Dead Sea (e.g., Sirota et al., 2016). In the context of our model, this particular role of temperature would be captured by the imposed convective flux.

5.2. Role of salinity-related feedbacks

In view of the already large number of parameters in our box model, we deliberately assumed the various fluxes of water and salt between the boxes to be independent of salinity. Here we discuss how any feedbacks would impact on our results.

Exchange is dependent on the density gradient at the strait – controlled by gateway dimensions (Simon and Meijer, 2015) and Mediterranean evaporative loss (Simon et al., 2017). Due to the neglect of temperature, salinity directly represents density. When salinity is still increasing (prior to steady state), the pressure gradient along the strait would increase and enhance exchange. The latter, in turn, would dampen the rise in basin salinity. Steady state results are not impacted by this feedback, because the final basin salinity is in balance with the prescribed outflux.

A higher salinity of a water body will reduce its activity, which lowers the rate of evaporation (Warren, 2016; see also Salhotra et al., 1985). Myers and Bonython (1958) approximated the effect linearly:

$$e = e_o * 1.0316 * (1 - 8.75 * 10^{-4} * S) \quad (4)$$

where e is the net evaporation affected by water salinity S and e_o corresponds to the initial value of e. This relationship shows that water at a salinity of ∼130–160 g/l (gypsum saturation) will cause a reduction in evaporation of ∼10% and water at a salinity of ∼350 g/l (halite saturation) of ∼28%. If we would account for the salinity-dependence of evaporation, stratification would be

weaker than now found for a given combination of the other controlling parameters (Fig. 3). Interestingly, below halite saturation this would result in lower surface salinity, thus increasing evaporation again.

We impose a constant convective flux (w), while in reality this depends on the density in the DWF-area relative to the density of the deep water. A larger density difference (i.e., larger salinity difference) would correspond to a larger w. Therefore, when both the DWF-box and deep box are close to halite saturation, a very low q would be the result, which would continue to decrease with time, making halite rain the dominant supplier of salt to the deep basin. In contrast, if the deep basin has a much lower salinity than the DWF-box (e.g., when c is low), stronger convection may be the case, which would re-distribute salt and in the extreme case even stop halite rain. This complex feedback loop again illustrates that a basin at halite saturation behaves very differently from the present Mediterranean.

If diffusivity (κ) would decrease with increasing stratification, the result would be to further increase stratification, demonstrating a positive feedback loop (compare Fig. 4 with 5). This would hold true up to the moment that diffusivity is so small that mixing is effectively turned off (compare supplementary Figs. S14C and G with S14D and H).

5.3. Consequences of the simple evaporite precipitation model

Warren (2016) shows that if marine water rises to a salt concentration of ~40–60 g/l, carbonates will be precipitated, followed by sulfates at ~130–160 g/l (e.g., gypsum, $CaSO_4$) and chlorides at ~340–360 g/l (e.g., halite, NaCl). Ideally, for each ionic salt pair a crystallization threshold would have to be introduced in the model. Whereas Topper and Meijer (2013) treated gypsum and halite separately, we only consider the formation of halite. An inclusion of a gypsum threshold in our model might lead to a slower increase in salinity than predicted now (from ~130–160 g/l onwards). As this would impact the DWF-box first, it might take the deep and surface slightly longer to reach this threshold. Once the threshold is reached by all boxes, no drastic additional effect is expected. Regarding the halite threshold, if salinity were allowed to rise beyond 350 g/l, the Deep or DWF-box would not force the system to a steady state as sharply as shown. This might allow the surface salinity to increase to higher values than predicted; however, also the other boxes will have higher salinities, which might balance and cause no significant effect on the stratification behaviour. Na^+ and Cl^- are by far the most prominent ions dissolved in marine water. Therefore, density is prominently dependent on dissolved halite. We argue that as a first pass our evaporite precipitation model is a fair approximation.

5.4. Limitations imposed by model geometry

The fact that the surface layer (outside the DWF-region) is represented by a single salinity is a simplification. In reality the salinity ranges from the Atlantic value (36 g/l) in the west, to a much elevated salinity adjacent to the DWF-box. This lateral variation would imply lateral variation in vertical stratification and could affect the strength of the exchange and the salinity in the DWF-box.

Representing the water column with only two layers is another imposed simplification. Again, the calculated mean salinities are likely to be more variable in reality. This implies that deep brines could have formed at even less extreme parameter values than found now. This representation could be improved by either adding more layers or by implementing the 1D advection–diffusion equation (e.g., Wåhlin and Cenedese, 2006). Although this would increase the vertical resolution, also other processes would need

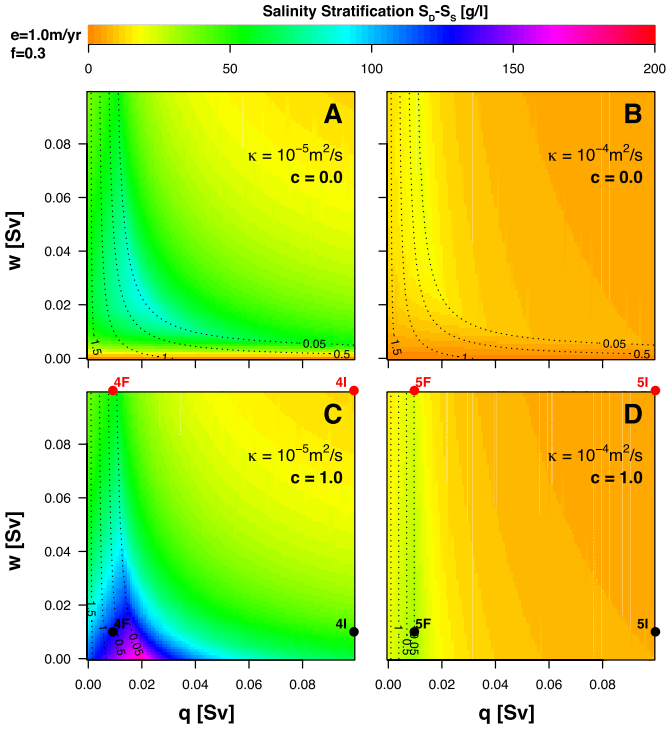

Fig. 9. Degree of stratification plotted for 4 sets (2 κ-values by 2 c-values) of 10^4 experiments for various w (y-axis) and q (x-axis). All other parameters are constant and set to $e = 1.0$ m/yr, $f = 0.3$ and $d = 160$ m. Contour lines indicate the halite sedimentation rate for the same parameter space. Red and black dots on panel C and D link to individual experiments presented in Figs. 4 and 5. Three equivalent figures are placed in the Supplementary Figs. S11–S13, which differ in e and f values. (For interpretation of the references to colour in this figure legend, the reader is referred to the web version of this article.)

to be considered in greater detail. For example the settling depth of convecting water would need to be parameterised.

Even in the light of these limitations regarding temperature, evaporite deposition and model geometry, our first order insights regarding the Mediterranean stratigraphy during the MSC hold true.

6. Conclusions

Our model analysis allows us to gain the first physics-based insight into the factors that determine the extent of water stratification of the Mediterranean Sea during the Messinian Salinity Crisis. A systematic sensitivity analysis shows under which conditions either a stratified or a mixed basin is expected. Considering the parameter space relevant for the Messinian Mediterranean, we conclude that a stratified water column may well have occurred, if the rate of deep-water formation was low while the area across which this happened was relatively large (both in comparison to the present day). In this case, synchronous formation of gypsum and halite could have occurred at different vertical levels within the basin. Halite sedimentation rate would be lower in the stratified case compared to a mixed basin, which would be in disagreement with the duration assigned to the halite in the stratigraphic consensus model of the MSC (Roveri et al., 2014a).

Acknowledgements

We thank Rinus Wortel for his constructive feedback on this manuscript and the MEDGATE team, particularly Frits Hilgen, for inspiring discussions on the Messinian Salinity Crisis and the Atlantic–Mediterranean exchange. Two anonymous referees are acknowledged for their careful reviews. The research leading to these

results has received funding from the People Programme (Marie Curie Actions) of the European Unions Seventh Framework Programme FP7/2007-2013/ under REA Grant Agreement No. 290201 MEDGATE.

Appendix A. Supplementary material

Supplementary material related to this article can be found online at https://doi.org/10.1016/j.epsl.2017.09.045.

References

Anati, D.A., 1997. The hydrography of a hypersaline lake. In: Oxford Monographs on Geology and Geophysics, vol. 36, pp. 89–103.

Béranger, K., Drillet, Y., Houssais, M.N., Testor, P., Bourdallé-Badie, R., Alhammoud, B., Bozec, A., Mortier, L., Bouruet-Aubertot, P., Crépon, M., 2010. Impact of the spatial distribution of the atmospheric forcing on water mass formation in the Mediterranean Sea. J. Geophys. Res., Oceans 115 (C12).

Bryden, H., Schroeder, K., Borghini, M., Vetrano, A., Sparnocchia, S., 2014. Mixing in the deep waters of the western Mediterranean. In: The Mediterranean Sea: Temporal Variability and Spatial Patterns, pp. 51–58.

Bryden, H.L., Stommel, H.M., 1984. Limiting processes that determine basic features of the circulation in the Mediterranean-Sea. Oceanol. Acta 7 (3), 289–296.

de Lange, G.J., Krijgsman, W., 2010. Messinian salinity crisis: a novel unifying shallow gypsum/deep dolomite formation mechanism. Mar. Geol. 275 (1), 273–277.

D'Ortenzio, F., Iudicone, D., de Boyer Montegut, C., Testor, P., Antoine, D., Marullo, S., Santoleri, R., Madec, G., 2005. Seasonal variability of the mixed layer depth in the Mediterranean Sea as derived from in situ profiles. Geophys. Res. Lett. 32 (12).

Feng, Y.E., Yankelzon, A., Steinberg, J., Reshef, M., 2016. Lithology and characteristics of the Messinian evaporite sequence of the deep Levant Basin, eastern Mediterranean. Mar. Geol. 376, 118–131.

Flecker, R., Krijgsman, W., Capella, W., de Castro Martíns, C., Dmitrieva, E., Mayser, J.P., Marzocchi, A., Modestu, S., Ochoa, D., Simon, D., Tulbure, M., van den Berg, B., van der Schee, M., de Lange, G., Ellam, R., Govers, R., Gutjahr, M., Hilgen, F., Kouwenhoven, T., Lofi, J., Meijer, P., Sierro, F.J., Bachiri, N., Barhoun, N., Alami, A.C., Chacon, B., Flores, J.A., Gregory, J., Howard, J., Lunt, D., Ochoa, M., Pancost, R., Vincent, S., Yousfi, M.Z., 2015. Evolution of the Late Miocene Mediterranean–Atlantic gateways and their impact on regional and global environmental change. Earth-Sci. Rev. 150, 365–392.

Gladstone, R., Flecker, R., Valdes, P., Lunt, D., Markwick, P., 2007. The Mediterranean hydrologic budget from a Late Miocene global climate simulation. Palaeogeogr. Palaeoclimatol. Palaeoecol. 251 (2), 254–267.

Grimm, R., Maier-Reimer, E., Mikolajewicz, U., Schmiedl, G., Müller-Navarra, K., Adloff, F., Grant, K.M., Ziegler, M., Lourens, L.J., Emeis, K.C., 2015. Late glacial initiation of Holocene eastern Mediterranean sapropel formation. Nat. Commun. 6.

Herrmann, M., Bouffard, J., Béranger, K., 2009. Monitoring open-ocean deep convection from space. Geophys. Res. Lett. 36 (3).

Jayne, S.R., 2005. September. Ocean Topography, Tides, Mixing, and the Earth's Climate. In: OCEANS 2005. Proceedings of MTS/IEEE. IEEE, pp. 1–4.

Johnson, H.L., Marshall, D.P., Sproson, D.A., 2007. Reconciling theories of a mechanically driven meridional overturning circulation with thermohaline forcing and multiple equilibria. Clim. Dyn. 29 (7–8), 821–836.

Lofi, J., Déverchère, J., Gaullier, V., Gillet, H., Gorini, C., Guennoc, P., Loncke, L., Maillard, A., Sage, F., Thinon, I., 2011. Seismic atlas of the Messinian Salinity Crisis markers in the Mediterranean and Black Seas, vol. 179. Société Géologique de France, pp. 1–72.

Lugli, S., Manzi, V., Roveri, M., Schreiber, C.B., 2010. The Primary Lower Gypsum in the Mediterranean: a new facies interpretation for the first stage of the Messinian salinity crisis. Palaeogeogr. Palaeoclimatol. Palaeoecol. 297 (1), 83–99.

Manzi, V., Gennari, R., Lugli, S., Roveri, M., Scafetta, N., Schreiber, B.C., 2012. High-frequency cyclicity in the Mediterranean Messinian evaporites: evidence for solar–lunar climate forcing. J. Sediment. Res. 82 (12), 991–1005.

Mariotti, A., Struglia, M.V., Zeng, N., Lau, K.M., 2002. The hydrological cycle in the Mediterranean region and implications for the water budget of the Mediterranean Sea. J. Climate 15 (13), 1674–1690.

Marzeion, B., Levermann, A., 2009. Stratification-dependent mixing may increase sensitivity of a wind-driven Atlantic overturning to surface freshwater flux. Geophys. Res. Lett. 36 (20).

Matthiesen, S., Haines, K., 2003. A hydraulic box model study of the Mediterranean response to postglacial sea-level rise. Paleoceanography 18 (4).

Meijer, P.T., Krijgsman, W., 2005. A quantitative analysis of the desiccation and refilling of the Mediterranean during the Messinian Salinity Crisis. Earth Planet. Sci. Lett. 240 (2), 510–520.

Meijer, P.T., 2006. A box model of the blocked-outflow scenario for the Messinian Salinity Crisis. Earth Planet. Sci. Lett. 248 (1), 486–494.

Meijer, P.T., 2012. Hydraulic theory of sea straits applied to the onset of the Messinian Salinity Crisis. Mar. Geol. 326, 131–139.

Mikolajewicz, U., Maier-Reimer, E., Crowley, T.J., Kim, K.Y., 1993. Effect of Drake and Panamanian gateways on the circulation of an ocean model. Paleoceanography 8 (4), 409–426.

Munk, W.H., 1966. Abyssal recipes. Deep-Sea Res. Oceanogr. Abstr. 13 (4), 707–730, Elsevier, August.

Myers, D.M., Bonython, C.W., 1958. The theory of recovering salt from sea-water by solar evaporation. J. Chem. Technol. Biotechnol. 8 (4), 207–219.

Ochoa, D., Sierro, F.J., Lofi, J., Maillard, A., Flores, J.A., Suárez, M., 2015. Synchronous onset of the Messinian evaporite precipitation: first Mediterranean offshore evidence. Earth Planet. Sci. Lett. 427, 112–124.

Pinardi, N., Masetti, E., 2000. Variability of the large scale general circulation of the Mediterranean Sea from observations and modelling: a review. Palaeogeogr. Palaeoclimatol. Palaeoecol. 158 (3), 153–173.

Rohling, E.J., Marino, G., Grant, K.M., 2015. Mediterranean climate and oceanography, and the periodic development of anoxic events (sapropels). Earth-Sci. Rev. 143, 62–97.

Rohling, E.J., Schiebel, R., Siddall, M., 2008. Controls on Messinian lower evaporite cycles in the Mediterranean. Earth Planet. Sci. Lett. 275 (1), 165–171.

Roveri, M., Flecker, R., Krijgsman, W., Lofi, J., Lugli, S., Manzi, V., Sierro, F.J., Bertini, A., Camerlenghi, A., De Lange, G., Govers, R., 2014a. The Messinian Salinity Crisis: past and future of a great challenge for marine sciences. Mar. Geol. 352, 25–58.

Roveri, M., Manzi, V., Bergamasco, A., Falcieri, F.M., Gennari, R., Lugli, S., Schreiber, B.C., 2014b. Dense shelf water cascading and Messinian canyons: a new scenario for the Mediterranean salinity crisis. Am. J. Sci. 314 (3), 751–784.

Roveri, M., Gennari, R., Lugli, S., Manzi, V., Minelli, N., Reghizzi, M., Riva, A., Rossi, M.E., Schreiber, B.C., 2016. The Messinian salinity crisis: open problems and possible implications for Mediterranean petroleum systems. Pet. Geosci. 22 (4), 283–290.

Ryan, W.B., 2008. Modeling the magnitude and timing of evaporative drawdown during the Messinian salinity crisis. Stratigraphy 5 (1), 227–243.

Salhotra, A.M., Adams, E.E., Harleman, D.R., 1985. Effect of salinity and ionic composition on evaporation: analysis of Dead Sea evaporation pans. Water Resour. Res. 21 (9), 1336–1344.

Schroeder, K., Garcia-Lafuente, J., Josey, S.A., 2012. Circulation of the Mediterranean Sea and its variability. In: Lionello, P. (Ed.), Mediterranean Climate: From Past to Future. Elsevier, Amsterdam, pp. 187–256.

Sevault, F., Somot, S., Alias, A., Dubois, C., Lebeaupin-Brossier, C., Nabat, P., Adloff, F., Déqué, M., Decharme, B., 2014. A fully coupled Mediterranean regional climate system model: design and evaluation of the ocean component for the 1980–2012 period. Tellus A 66.

Simon, D., Meijer, P., 2015. Dimensions of the Atlantic–Mediterranean connection that caused the Messinian Salinity Crisis. Mar. Geol. 364, 53–64.

Simon, D., Marzocchi, A., Flecker, R., Lunt, D.J., Hilgen, F.J., Meijer, P.T., 2017. Quantifying the Mediterranean freshwater budget throughout the late Miocene: new implications for sapropel formation and the Messinian Salinity Crisis. Earth Planet. Sci. Lett. 472, 25–37.

Sirota, I., Arnon, A., Lensky, N.G., 2016. Seasonal variations of halite saturation in the Dead Sea. Water Resour. Res. 52 (9), 7151–7162.

Sonnenfeld, P., Finetti, I., 1985. Messinian evaporites in the Mediterranean: a model of continuous inflow and outflow. In: Geological Evolution of the Mediterranean Basin. Springer, New York, pp. 347–353.

Soto-Navarro, J., Criado-Aldeanueva, F., García-Lafuente, J., Sánchez-Román, A., 2010. Estimation of the Atlantic inflow through the Strait of Gibraltar from climatological and in situ data. J. Geophys. Res., Oceans 115 (C10).

Thorpe, S.A., 2005. The Turbulent Ocean. Cambridge University Press.

Topper, R.P.M., Meijer, P.T., 2013. A modeling perspective on spatial and temporal variations in Messinian evaporite deposits. Mar. Geol. 336, 44–60.

Topper, R.P.M., Meijer, P.T., 2015. Changes in Mediterranean circulation and water characteristics due to restriction of the Atlantic connection: a high-resolution ocean model. Clim. Past 11 (2), 233–251.

Tsimplis, M.N., Zervakis, V., Josey, S.A., Peneva, E.L., Struglia, M.V., Stanev, E.V., Theocharis, A., Lionello, P., Malanotte-Rizzoli, P., Artale, V., Tragou, E., 2006. Changes in the oceanography of the Mediterranean Sea and their link to climate variability. In: Developments in Earth and Environmental Sciences, vol. 4, pp. 227–282.

Tziperman, E., Speer, K., 1994. A study of water mass transformation in the Mediterranean Sea: analysis of climatological data and a simple three-box model. Dyn. Atmos. Ocean. 21 (2–3), 53–82.

Wåhlin, A.K., Cenedese, C., 2006. How entraining density currents influence the stratification in a one-dimensional ocean basin. Deep-Sea Res., Part 2, Top. Stud. Oceanogr. 53 (1), 172–193.

Yoshimura, T., Kuroda, J., Lugli, S., Tamenori, Y., Ogawa, N.O., Jiménez-Espejo, F.J., Isaji, Y., Roveri, M., Manzi, V., Kawahata, H., Ohkouchi, N., 2016. An X-ray spectroscopic perspective on Messinian evaporite from Sicily: sedimentary fabrics, element distributions, and chemical environments of S and Mg. Geochem. Geophys. Geosyst. 17 (4), 1383–1400.

Warren, J.K., 2016. Evaporites: A Geological Compendium. Springer.